

# Transcervical Ultrasound Image Guidance System for Transoral Robotic Surgery

Wanwen Chen<sup>1\*</sup>, Megha Kalia<sup>1</sup>, Qi Zeng<sup>1</sup>, Emily H.T. Pang<sup>2</sup>, Razeyeh Bagherinasab<sup>1</sup>, Thomas D. Milner<sup>3</sup>, Farahna Sabiq<sup>2</sup>, Eitan Prisman<sup>3</sup> and Septimiu E. Salcudean<sup>1</sup>

<sup>1\*</sup>Department of Electrical and Computer Engineering, The University of British Columbia, Vancouver, BC, Canada.

<sup>2</sup>Department of Radiology, Vancouver General Hospital, Vancouver, BC, Canada.

<sup>3</sup>Department of Otolaryngology, Vancouver General Hospital, Vancouver, BC, Canada.

\*Corresponding author(s). E-mail(s): [wanwenc@ece.ubc.ca](mailto:wanwenc@ece.ubc.ca);

## Abstract

**Purpose:** Trans-oral robotic surgery (TORS) using the da Vinci surgical robot is a new minimally-invasive surgery method to treat oropharyngeal tumors, but it is a challenging operation. Augmented reality (AR) based on intra-operative ultrasound (US) has the potential to enhance the visualization of the anatomy and cancerous tumors to provide additional tools for decision-making in surgery.

**Methods:** We propose and carry out preliminary evaluations of a US-guided AR system for TORS, with the transducer placed on the neck for a transcervical view. Firstly, we perform a novel MRI-transcervical 3D US registration study. Secondly, we develop a US-robot calibration method with an optical tracker and an AR system to display the anatomy mesh model in the real-time endoscope images inside the surgeon console.

**Results:** Our AR system reaches a mean projection error of 26.81 and 27.85 pixels for the projection from the US to stereo cameras in a water bath experiment. The average target registration error for MRI to 3D US is 8.90 mm for the 3D US transducer and 5.85 mm for freehand 3D US, and the average distance between the vessel centerlines is 2.32 mm.

**Conclusion:** We demonstrate the first proof-of-concept transcervical US-guided AR system for TORS and the feasibility of transcervical 3D US-MRI registration. Our results show that transcervical 3D US is a promising technique for TORS image guidance.

**Keywords:** Transoral robotic surgery, 3D ultrasound, Surgical augmented reality, MRI-US registration

## 1 Introduction

The American Cancer Society estimates that there will be about 54,000 new cases and 11,230 deaths from cancer of the oral cavity and pharynx (throat) in the United States in 2022 [1]. The incidence rates increased by 0.8% per year from 2009 to 2018 while the mortality rate increased by 0.4% per year from 2010 to 2019 [1]. Oropharyngeal cancer is one of the commonest types of head and neck cancer, and was traditionally treated with either open surgery or radiotherapy. TORS is a new minimally invasive technique that allows surgeons to remove oropharyngeal cancers with fewer side effects, to help preserve the function of patients after treatment [2].

TORS, however, is challenging because surgeons need to work in a severely constrained environment, through the patient's mouth, superior to the retracted tongue, without haptic feedback, requiring a profound knowledge of the oropharynx and parapharynx anatomy [3]. Image-guidance has the potential to improve TORS through anatomy and cancer visualization.

Current TORS image guidance approaches mostly use cross-sectional images to visualize preoperative computerized tomography (CT) or magnetic resonance imaging (MRI) [4–6]. CT is the most common intraoperative imaging modality. Comparisons between preoperative and intraoperative CT show that the former is insufficient to visualize the deformed anatomy, while the latter can improve fiducial localization accuracy and task efficiency [7, 8]. A tri-planar CT-based surgical navigation system is presented in [9]. Deformable registration from preoperative images to cone-beam CT to augment anatomy structures and surgical planning data in stereoscopic video is presented in [10]. However, intra-operative CT does introduce radiation risk.

US can provide real-time intra-operative imaging for TORS without radiation. In most previous research, the US transducer was placed in the patient's oral cavity. Intra-oral US interferes with the TORS robot tools. These must either be removed [11, 12] or a miniaturized US transducer with limited scanning range must be used instead [13–15]. Shen [16] has proposed an intraoral 3D US-guided AR system for transoral surgery, using a head-mounted display with AR displaying the tumor model segmented in the 3D US to guide the tumor resection in an *ex vivo* tongue. To the best of our knowledge, this is the most similar system to our study, but it does not solve the problem of removing robot tools from the patient's mouth to insert the US transducer. Therefore, to

mitigate this problem, we explore a different US transducer placement whose feasibility for TORS is still unknown.

Transcervical US, which places the US transducer outside the patient's neck, can provide continuous US imaging during TORS. Transcervical 3D US has been used in head and neck procedures such as neck fine-needle puncture [17] and neck tumor dissection [18], as well as in oral cancer diagnosis [19–21], but its feasibility in TORS has not been studied.

While US is accessible and safe, US images are usually harder to interpret than CT or MRI. Furthermore, US imaging is subject to a severe tradeoff between imaging resolution and depth; larger depths require lower frequencies for penetration and therefore will have lower image resolution. US-preoperative image registration can combine the benefits of different image modalities to assist surgical planning. In particular, MRI provides high soft-tissue contrast and cancer imaging that can be exploited by MRI-US registration. MRI-US registration and real-time US have been used in other surgeries such as prostatectomy [22, 23]. We hypothesize that they can also be applied to TORS, but the feasibility of MRI-3D US registration in the oropharynx is not well studied. Chen *et al.* [24] conducted a feasibility study of MRI-3D US registration for TORS; their results show that the 3D images acquired by a low-frequency 3D transducer might not have sufficient resolution for image registration.

In this research, we propose a proof-of-concept AR system for TORS utilizing transcervical 3D US. To the best of our knowledge, our contributions include: (1) the first work evaluating the feasibility of MRI and freehand 3D US registration in the oropharynx, (2) the first work comparing the differences between two types of 3D US of the oropharyngeal region; (3) the first AR system utilizing both US and MRI in TORS.

## 2 Materials and Methods

Fig. 1 shows the proposed US-guided AR workflow. In the planning stage, preoperative MRI and US are collected for surgical planning and feasibility evaluation of US-guided TORS. Just before surgery, the AR system is calibrated and a preoperative freehand US scanning and MRI-US registration are carried out for an initial AR display of the anatomy model. During surgery, the patient's tongue is retracted, and the surgeon can use the US transducer to scan the tumor side and visualize the US. A US-to-US intraoperative-to-preoperative registration generates the deformation field to update the anatomy model in AR. In this preliminary study, we evaluate the feasibility of the first and the second stage: MRI-US registration and system calibration.

### 2.1 System Hardware

Fig. 2 shows the components of our system. The da Vinci surgical system (Intuitive Surgical, Sunnyvale, CA) includes a patient side cart and a surgeon's console, which provides the surgeon with an endoscope view. The US system is a BK3500 with a 14L3 linear 2D transducer (BK Medical, Burlington, MA).

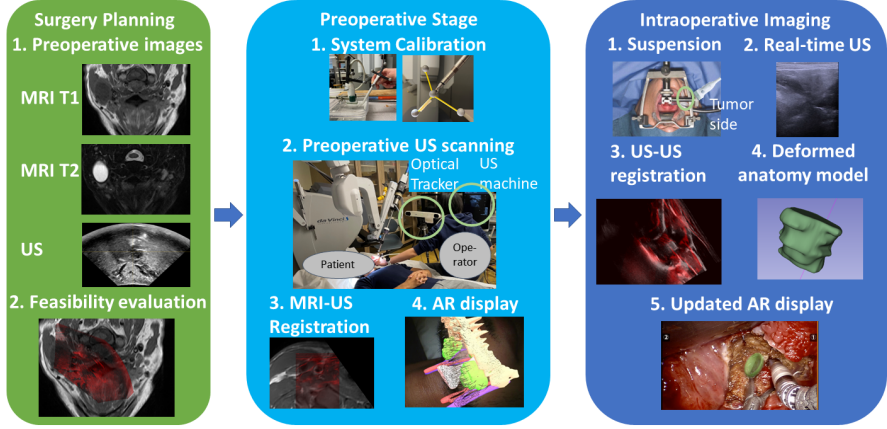


**Fig. 1:** The proposed workflow of the AR-guided TORS.

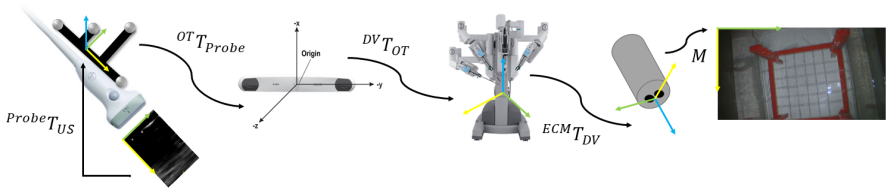


**Fig. 2:** The hardware systems and the transformations in the system calibration to transform from the US image frame to the camera image frame.

A Polaris Spectra (Northern Digital, ON, Canada) tracks the US transducer. To enable US probe maneuvering by the surgeon using the da Vinci's third manipulating arm, we designed a novel 3D-printed US transducer holder that allows the surgeon to grasp and move it with the da Vinci ProGrasp in the console, as in Fig. 3a.

## 2.2 System Calibration

Eq. 1 shows the transformations needed to project the US volume onto the camera image ( ${}^i T_{US}$ ). The endoscopic camera (ECM) location  ${}^{DV} T_{ECM}$  can be read from the da Vinci robot API and the marker on the probe can be tracked by the optical tracker  ${}^{OT} T_{Probe}$ . Therefore, the system calibration requires us to find the transformation from US image to the marker on the probe  ${}^{Probe} T_{US}$ , from optical tracker to robot  ${}^{DV} T_{OT}$ , and the camera projection matrix  $M$ .

$${}^i T_{US} = M {}^{ECM} T_{DV} {}^{DV} T_{OT} {}^{OT} T_{Probe} {}^{Probe} T_{US} \quad (1)$$

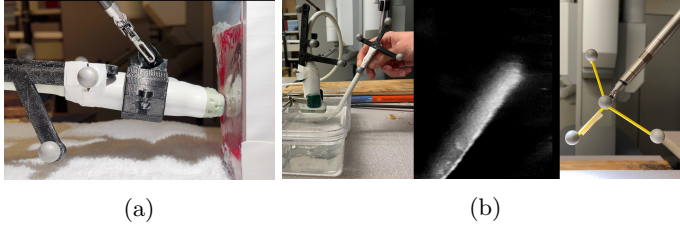


**Fig. 3:** (a) Image showing the 3D-printed holder and how the robot grasps the US transducer. (b) Images of the system calibration. From left to right: (1) the tracked US transducer and stylus; (2) a US image of the stylus tip; (3) a robot tool holding our designed marker for robot-tracker calibration.

**US to Optical Tracker Calibration.** We used the PLUS toolkit [25] and SlicerIGT [26] for US-tracker calibration. A 3D-printed marker is attached to the US transducer to localize it in the tracker coordinate frame  $OT$ . PLUS enables collecting time-synchronized transducer locations and US images. We first run the temporal calibration to correct the time offset, then we collect a tracked US video sequence imaging the tip of a tracked stylus pointer. The transformation  $^{Stylus}T_{tip}$  is known after a pivot calibration. We then use the fiducial registration in 3D Slicer to manually select the stylus tip location in the US images and to estimate a similarity transformation  $^{Probe}T_{US}$

$$^{Probe}T_{US} = \arg \min_T \| {}^{OT}T_{Stylus} {}^{Stylus}T_{tip} - {}^{OT}T_{Probe} T^{US}T_{tip} \|_2$$

where  $Probe$  is the coordinate frame of the marker attached to the US transducer.

**Robot to Optical Tracker Calibration.** We attach a customized marker with a known marker coordinate origin to the robot tooltip and collect the corresponding points in the tracker and robot coordinate frames. We then estimate a rigid transformation between the corresponding points for  $^{OT}T_{DV}$ .

$$^{OT}T_{DV} = \arg \min_T \| {}^{OT}T_{marker} - T^{DV}T_{Tip} \|_2$$

**Camera Projection Matrix Calibration.** We use the camera projection calibration algorithm in [23] to estimate the camera projection matrix  $M$ , which includes the hand-eye calibration matrix (the transformation from ECM to the camera world coordinate system) and the camera intrinsic matrix. The algorithm automatically detects fourteen key points on the robot tool in the robot and image coordinates. By moving the robot tool we will get corresponding spatial 3D and 2D points to estimate  $M$ .

## 2.3 MRI-3D US Registration

For MRI-US registration we need to find a spatial transformation  $^{MRI}T_{US}$ . After the registration, we can map the MRI volume or the anatomy model

**Table 1:** Mean projection error of the points projected from US to the camera.

	Left Camera	Right Camera
Projection Error (pixel)	27.85 ± 10.52	26.81 ± 9.03

generated from the MRI to the camera image by  ${}^i T_{MRI} = {}^i T_{US} {}^{US} T_{MRI}$ . To simplify the transformation in the AR system, we assume  ${}^{MRI} T_{US}$  is an affine transformation. We first manually rigidly pre-register the 3D US volume and axial T1 MRI based on the US transducer position and anatomy structures. Other MRI sequences can be used during this process. The Linear Correlation of Linear Combination (LC2)-based optimization [27] (ImFusion GmbH, Munich, Germany) is used to refine the affine transformation  ${}^{US} T_{MRI}$ . We evaluate the MRI-US registration for two different types of 3D US. We first used a 3D US transducer (xMATRIX X6-1, Philips Healthcare, Bothell, WA) to acquire 3D US of the oropharynx in five healthy volunteers and four patients with oropharyngeal cancer, referring the scanning protocol in Coquia *et al.* [28]. We then used the BK3500 US machine, 14L3 linear transducer and the optical tracker in Section 2.1 and PLUS to record the tracked US image sequences and reconstruct freehand 3D US for three healthy volunteers.

## 3 Experiments and Results

### 3.1 System Evaluation

To evaluate the accuracy of the robot-tracker calibration, we collected 100 pairs of points and used 50% to estimate  ${}^{DV} T_{OT}$  and 50% for testing. The mean projection error is 1.73 mm in the training data and 1.84 mm in the test data. We then measure the stylus-based calibration error by using 25 pairs of points to estimate  ${}^{probe} T_{US}$  and the mean projection error is 0.59 mm. We used another 17 fiducial pairs for testing and the mean projection error is 0.78 mm.

We evaluated the system accuracy  ${}^i T_{US}$  in a water-bath experiment, whose workflow is in Fig. 4. We used a 3D-printed structure and nylon wires to build 25 grid points, with nominal grid size of 10 mm, within the accuracy of the 3D printer. We used freehand 3D US to image the grids and thresholded by intensity to segment the wires. We then projected the wires from the US to the camera and labeled the grids. We put the structure in three different locations and collected 75 data points. The image size is  $540 \times 960$ , and the mean projection error is in Table 1. The final system demonstration is in Fig. 5, projecting the anatomy models segmented from the MRI to the camera with  ${}^i T_{MRI}$  on a human subject. For the mannequin, we used the US to scan the surface and we registered the surface with the skin surface in MRI.

### 3.2 Preliminary Evaluation of MRI-US Registration

MRI was acquired using a 3T Philips Elition MRI (Philips Healthcare, Bothell, WA) for healthy volunteers, with axial resolution in T1 images of 0.35 to 0.45 mm in the transverse plane and 3.6 to 4.5 mm in the axial direction.

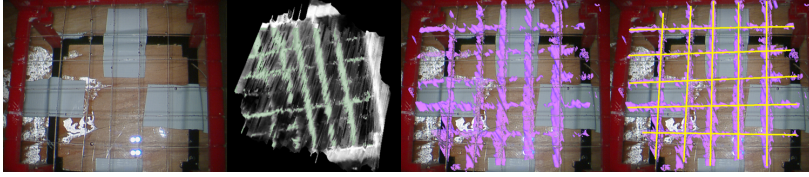


**Fig. 4:** The water-bath experiment. From left to right: (1) original camera image; (2) 3D freehand US volume and wire segmentation; (3) projected segmentation in the camera image; (4) the labeled wires.

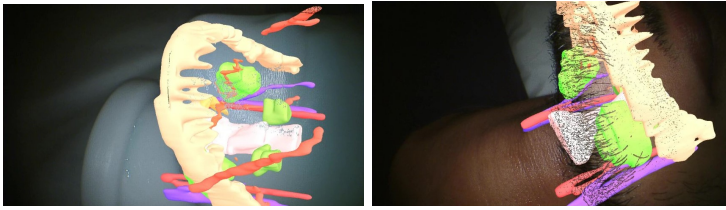


**Fig. 5:** Images of the AR guidance system viewed in the camera frame.

**Table 2:** The target registration error (TRE) (in mm) for patients or healthy volunteers (HV), and the average TRE for all the cases [24].

Plane	Transverse		Axial		Total	
TRE (mm)	HVs	Patients	HVs	Patients	HVs	Patients
By Group	7.29±6.50	6.45±3.47	3.04±4.33	5.94±6.23	8.26±7.41	9.63±5.91
All	6.89±5.32		4.39±5.49		8.90±6.79	

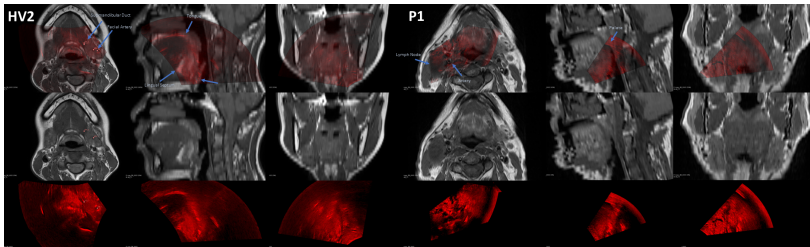
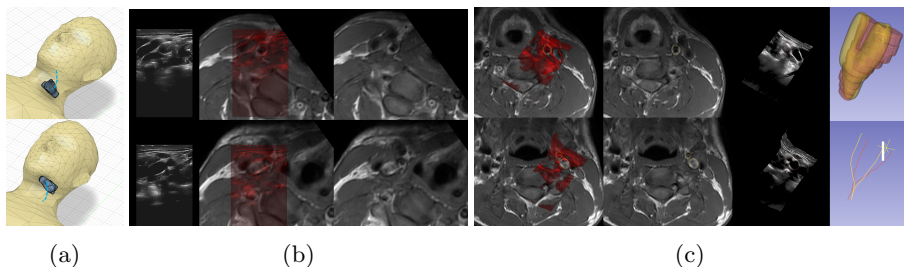
For participants with oropharyngeal cancer a Siemens Magnetom Espree 1.5T MRI (Siemens Healthcare, Erlangen, Germany) was used with a resolution of 0.375 mm in the transverse plane and 3.6 mm in the axial direction. A radiologist (EP) manually selected anatomical landmarks in US and MRI to evaluate the target registration error (TRE).

For the 3D transducer-collected US, the elevation angle is 45 – 90° and the image depth is 7-9 cm. The frequency range is 1-6MHz. The spatial resolution is around  $0.3 \times 0.2 \times 0.4\text{mm}^3$ . The TRE for MRI-3D probe-collected US is in Table 2 and Fig. 6 shows two registration examples. For freehand 3D US, the image depth is 6 cm at 9 MHz and the US volume spacing is 0.1 mm for three axes. We scanned the participant’s neck from the common carotid to the submandibular gland, as in Fig. 7. We segmented the carotids that appeared in both MRI and US and used Slicer Vascular Modeling Toolkit [29] to extract the centerlines. The TRE and the average distance between the centerlines are in Table 3: we first interpolate each vessel branch into 1000 points and then calculate the average distance between the corresponding points.



**Table 3:** The target registration error (TRE) and the average distance of the vessel centerlines for MRI-freehand 3D US registration.

	TRE (mm)			Average Distance (mm)
	Transverse	Axial	Total	
HV1	3.78±0.47	5.40±1.80	6.63±1.73	2.15
HV2	3.18±0.84	0.89±1.56	3.61±1.01	2.13
HV3	5.48±2.15	3.45±2.81	7.33±0.86	2.67
Average	4.34±1.88	2.88±2.79	5.85±2.05	2.32±0.25

**Fig. 6:** Examples of MRI-US registration using a 3D US probe [24].**Fig. 7:** Examples of MRI-freehand 3D US registration. (a) the scanning trajectory (models from [25]); (b) examples of 2D US, MRI-US overlay and re-sliced MRI; (c) MRI-US overlay of the reconstructed 3D US, MRI, re-sliced US, vessel segmentation and centerlines (yellow: MRI, red: US).

## 4 Discussion

We evaluate the accuracy of the system calibration in different steps. The US-tracker calibration and the robot-tracker calibration achieve a promising performance, and the water bath experiment shows that our system achieves comparative results with the previous system [23] with an additional optical tracker. Compared with the previous system, our system provides more degrees of freedom for the US transducer. This calibration technique can also be easily generalized to US guidance for other surgeries. The final system accuracy from the US to the camera is approximately 27 pixels, or 2.5% of the image diagonal. This error can be introduced by the calibration error and noise in the optical



tracking, and the wire segmentation and point labeling error in the freehand US. Wire segmentation is difficult because the wires cause artifacts in the US images and the noise in tracking introduces jitter in the reconstructed US.

We evaluate the feasibility of MRI-US registration for two different 3D US. The 3D transducer with low frequency can image the deeper oropharyngeal region, making the tongue surface and larynx easily visible for pre-registration. However, the details of the oropharynx are not clear, making the refinement and evaluation difficult. Freehand 3D US with higher frequency provides more details in the near-surface region and can scan a broader region. The common carotid artery, external carotid artery, and internal carotid artery are reliable landmarks for MRI-freehand 3D US registration. A future improvement is to detect these vessels automatically, with classical or learning-based techniques and use anatomy prior for pre-registration [30]. However, freehand 3D US has the disadvantage that the marker must be visible to the optical tracker during the scanning, making the process more complicated. The tracking reliability can be improved by better device space arrangement and careful marker design.

We find that the tissue deformation introduced by the forces applied on the participants during the US scanning increase the registration difficulty and error, and the visual offset in the AR display. Fig. 5 shows that the anatomy displayed on the mannequin is more realistic than on the human because the mannequin has a non-deformable surface that is similar to MRI. The participant's poses are different in MRI and US scanning, and their tissue is deformable, making the registration less accurate. In a real surgery scene, the deformation will be more severe because the tongue is retracted. However, for the surgeon to recall where the vessels are located presents an additional mental load because it is complicated and patient-dependent. Therefore, even with the visual offset, our AR display can be valuable to surgical decisions intraoperatively. This result also demonstrates the importance of real-time US to provide intraoperative information. A future improvement is to use deformable registration to improve registration accuracy, and also explore the feasibility of intraoperative US-preoperative US registration to correct the anatomy model.

## 5 Conclusion

We demonstrate the first proof-of-concept for a transcervical US-guided AR system for TORS. We conduct a feasibility study of transcervical 3D US-MRI registration for two different types of 3D US, showing that 3D US has the potential to visualize the anatomy intraoperatively. We propose a new AR system for TORS and evaluate the system accuracy. Our results show that 3D US transcervical imaging is a promising approach for image guidance in TORS.

**Acknowledgments.** We would like to thank the financial support from the Natural Sciences and Engineering Research Council of Canada (NSERC) and the Charles Laszlo Chair in Biomedical Engineering held by Dr. Salcudean. We would like to thank David Black, Nicholas Ranga and Angela Li for their help in CAD design.

## Declarations

- Competing interests: The authors have no conflicts of interest.
- Ethics approval: Institutional ethics approval was obtained for this study. All procedures in studies involving human participants were in accordance with the ethical standards of the institutional and national research committee.
- Consent to participate: Informed consent was obtained from all individual participants in the study.
- Data and code availability: Data and code are not publicly available.

## References

- [1] Siegel, R.L., Miller, K.D., Fuchs, H.E., Jemal, A., *et al.*: Cancer statistics, 2022. *Ca Cancer J Clin* **72**(1), 7–33 (2022)
- [2] Chow, L.Q.: Head and neck cancer. *New England Journal of Medicine* **382**(1), 60–72 (2020)
- [3] Moore, E.J., Janus, J., Kasperbauer, J.: Transoral robotic surgery of the oropharynx: clinical and anatomic considerations. *Clinical Anatomy* **25**(1), 135–141 (2012)
- [4] Desai, S.C., Sung, C.-K., Genden, E.M.: Transoral robotic surgery using an image guidance system. *The Laryngoscope* **118**(11), 2003–2005 (2008)
- [5] Pratt, P., Arora, A.: Transoral robotic surgery: image guidance and augmented reality. *ORL* **80**(3-4), 204–212 (2018)
- [6] Chan, J.Y., Holsinger, F.C., Liu, S., Sorger, J.M., Azizian, M., Tsang, R.K.: Augmented reality for image guidance in transoral robotic surgery. *Journal of Robotic Surgery* **14**(4), 579–583 (2020)
- [7] Ma, A.K., Daly, M., Qiu, J., Chan, H.H., Goldstein, D.P., Irish, J.C., de Almeida, J.R.: Intraoperative image guidance in transoral robotic surgery: A pilot study. *Head & Neck* **39**(10), 1976–1983 (2017)
- [8] Kahng, P.W., Wu, X., Ramesh, N.P., Pastel, D.A., Halter, R.J., Paydarfar, J.A.: Improving target localization during trans-oral surgery with use of intraoperative imaging. *International Journal of Computer Assisted Radiology and Surgery* **14**(5), 885–893 (2019)
- [9] Shi, Y., Lou, Y., Shirai, I., Wu, X., Paydarfar, J.A., Halter, R.J.: Surgical navigation system for image-guided transoral robotic surgery: a proof of concept. In: *Medical Imaging 2022: Image-Guided Procedures, Robotic Interventions, and Modeling*, vol. 12034, pp. 43–48 (2022). SPIE

- [10] Liu, W.P., Richmon, J.D., Sorger, J.M., Azizian, M., Taylor, R.H.: Augmented reality and cone beam ct guidance for transoral robotic surgery. *Journal of robotic surgery* **9**(3), 223–233 (2015)
- [11] Goepfert, R.P., Liu, C., Ryan, W.R.: Trans-oral robotic surgery and surgeon-performed trans-oral ultrasound for intraoperative location and excision of an isolated retropharyngeal lymph node metastasis of papillary thyroid carcinoma. *American journal of otolaryngology* **36**(5), 710–714 (2015)
- [12] Clayburgh, D.R., Byrd, J.K., Bonfili, J., Duvvuri, U.: Intraoperative ultrasonography during transoral robotic surgery. *Annals of Otolology, Rhinology & Laryngology* **125**(1), 37–42 (2016)
- [13] Liu, W.P., Holsinger, F.C., Vendra, V.: Abstract b29: Intraoperative identification of critical vascular landmarks of the lateral oropharynx and tongue base using transoral robotic ultrasound (torus). *Clinical Cancer Research* **26**(12\_Supplement\_2), 29–29 (2020)
- [14] Green, E.D., Paleri, V., Hardman, J.C., Kerawala, C., Riva, F.M., Jaly, A.A., Ap Dafydd, D.: Integrated surgery and radiology: trans-oral robotic surgery guided by real-time radiologist-operated intraoral ultrasound. *Oral and Maxillofacial Surgery* **24**(4), 477–483 (2020)
- [15] Chang, C.-C., Wu, J.-L., Hsiao, J.-R., Lin, C.-Y.: Real-time, intraoperative, ultrasound-assisted transoral robotic surgery for obstructive sleep apnea. *The Laryngoscope* **131**(4), 1383–1390 (2021)
- [16] Shen, J.: Framework for ultrasonography-based augmented reality in robotic surgery: application to transoral surgery and gastrointestinal surgery. PhD thesis, Université Rennes 1 (2019)
- [17] SCHIPPER, J., WOERN, H.: An ultrasound-based navigation system for minimally invasive neck surgery. *Medicine Meets Virtual Reality 21: NextMed/MMVR21* **196**, 36 (2014)
- [18] Snyder, L.A., McDougall, C.G., Spetzler, R.F., Zabramski, J.M.: Neck tumor dissection improved with 3-dimensional ultrasound image guidance: technical case report. *Operative Neurosurgery* **10**(1), 183–189 (2014)
- [19] Klimek, L., Schreiber, J., Amedee, R.G., Mann, W.J.: Three-dimensional ultrasound evaluation in the head and neck. *Otolaryngology–Head and Neck Surgery* **118**(2), 267–271 (1998)
- [20] Rebol, J.: Volume determination of oral cavity tumors by 3-dimensional ultrasonography. *Journal of oral and maxillofacial surgery* **66**(11), 2296–2301 (2008)

- [21] Hong, S.-F., Lai, Y.-S., Lee, K.-W., Chen, M.-K.: Efficiency of three-dimensional doppler ultrasonography in assessing nodal metastasis of head and neck cancer. *European Archives of Oto-Rhino-Laryngology* **272**, 2985–2991 (2015)
- [22] Mathur, P., Samei, G., Tsang, K., Lobo, J., Salcudean, S.: On the feasibility of transperineal 3d ultrasound image guidance for robotic radical prostatectomy. *International journal of computer assisted radiology and surgery* **14**(6), 923–931 (2019)
- [23] Kalia, M., Avinash, A., Navab, N., Salcudean, S.: Preclinical evaluation of a markerless, real-time, augmented reality guidance system for robot-assisted radical prostatectomy. *International Journal of Computer Assisted Radiology and Surgery* **16**(7), 1181–1188 (2021)
- [24] Chen, W., Zeng, Q., Milner, T.D., Bagherinasab, R., Sabiq, F., Prisman, E., Pang, E.H.T., Salcudean, S.E.: Feasibility of mri-us registration in oropharynx for transoral robotic surgery. In: *Accepted by Medical Imaging 2023: Image-Guided Procedures, Robotic Interventions, and Modeling* (2023). SPIE
- [25] Lasso, A., Heffter, T., Rankin, A., Pinter, C., Ungi, T., Fichtinger, G.: Plus: Open-source toolkit for ultrasound-guided intervention systems. *IEEE Transactions on Biomedical Engineering* (10), 2527–2537 (2014)
- [26] Ungi, T., Lasso, A., Fichtinger, G.: Open-source platforms for navigated image-guided interventions. *Medical image analysis* **33**, 181–186 (2016)
- [27] Wein, W., Ladikos, A., Fuerst, B., Shah, A., Sharma, K., Navab, N.: Global registration of ultrasound to mri using the lc 2 metric for enabling neurosurgical guidance. In: *International Conference on Medical Image Computing and Computer-Assisted Intervention*, pp. 34–41 (2013). Springer
- [28] Coquia, S.F., Hamper, U.M., Holman, M.E., DeJong, M.R., Subramaniam, R.M., Aygun, N., Fakhry, C.: Visualization of the oropharynx with transcervical ultrasound. *American Journal of Roentgenology* **205**(6), 1288–1294 (2015)
- [29] Hähn, D.: Integration of the vascular modeling toolkit in 3d slicer. PhD thesis, Citeseer (1909)
- [30] Zeng, Q., Mohammed, S., Pang, E.H., Schneider, C., Honarvar, M., Lobo, J., Hu, C., Jago, J., Ng, G., Rohling, R., *et al.*: Learning-based us-mr liver image registration with spatial priors. In: *International Conference on Medical Image Computing and Computer-Assisted Intervention*, pp. 174–184 (2022). Springer